Scrinzi's Laguerre DVR for exterior complex scaling

CWM September 2017, FY added notes on radial Poisson solve
for two-electron integrals, June 2018, CWM modifications July, 2018

Derives the working equations for putting a Laguerre-Radau element as the last element for an ECS calculation following ideas in Scrinzi's paper on using such a DVR in time-dependent calculations in the velocity gauge [1]. Numerical tests verify the working equations. The bottom line seems to be that adding the Laguerre element requires substantially fewer points to converge the cross section at low energies than does the addition of Gauss-Lobatto elements.

I. LAGUERRE DVR FOR THE SCHRÖDINGER EQUATION ON THE *REAL* INTERVAL $[0,\infty)$

We will first consider the radial Schrödinger equation for r times the radial wave function,

$$\left(-\frac{1}{2\mu}\frac{d^2}{dr^2}+\frac{l(l+1)}{2\mu r^2}+V(r)\right)\psi(r)=E\psi(r) \tag{1}$$

where we will expand $\psi(r)$ in a set of functions that are the usual DVR canonical functions

$$\psi(r)=\sum_n c_n\chi_n(r) \tag{2}$$

where

$$\begin{aligned}\chi_n(r)&=e^{-\alpha r}\tilde{\chi}_n(r)\\ \tilde{\chi}_n(r)&=\frac{1}{\sqrt{w_n}}\prod_{i\neq n}^{N}\frac{r-r_i}{r_n-r_i}\end{aligned} \tag{3}$$

The points r_i and weights w_i are to be defined using Gauss-Radau Laguerre quadrature such that these DVR functions will be orthonormal on the interval when the overlap is defined by

$$\begin{aligned}S_{n,m}&=\int_0^\infty \chi_n(r)\chi_m(r)dr\\ &=\int_0^\infty \tilde{\chi}_n(r)\tilde{\chi}_m(r)e^{-2\alpha r}dr\\ &\approx\sum_i \tilde{\chi}_n(r_i)\tilde{\chi}_m(r_i)w_i=\delta_{n,m}\end{aligned} \tag{4}$$

when the integral is done by Gauss-Laguerre quadrature in r. To define the weights and points we note the definition of Gauss-Laguerre quadrature is

$$\begin{aligned}\int_0^\infty f(x)e^{-x}dx&=\sum_i^N W_i f(x_i)+\mathcal{O}(f^{(2N)}(\xi))\\ 0<\xi<\infty&\end{aligned} \tag{5}$$

so it exactly integrates polynomials of order $2N-1$ or less time the exponential weight function. Gauss-Radau Laguerre quadrature with the left most point fixed ($x_1=0$) has a remainder of order $\mathcal{O}(f^{(2N)}(\xi))$ and exactly integrates polynomials of order $2n-2$. We want the integral

$$\int_0^\infty f(r)e^{-2\alpha r}dr\approx\sum_i^N w_i f(r_i) \tag{6}$$

so we make the change of variable $x=2\alpha r$ to get

$$\begin{aligned}&\int_0^\infty f(r)e^{-2\alpha r}dr=\\ &\int_0^\infty f(x/2\alpha)e^{-x}dx/2\alpha\approx\frac{1}{2\alpha}\sum_i^N W_i f(x_i/2\alpha)\\ &=\sum_i^N w_i f(r_i)\\ &r_i=x_i/2\alpha\\ &w_i=W_i/2\alpha\end{aligned} \tag{7}$$

Matrix elements of the operators are then defined as follows. For the potential and centrifugal potential

$$\begin{aligned}V_{n,m}&=\int_0^\infty \chi_n(r)V(r)\chi_m(r)dr\\ &=\int_0^\infty \tilde{\chi}_n(r)V(r)\tilde{\chi}_m(r)e^{-2\alpha r}dr\\ &\approx\sum_i w_i\ \tilde{\chi}_n(r_i)V(r_i)\tilde{\chi}_m(r_i)=\delta_{n,m}V(r_n)\end{aligned} \tag{8}$$

where to derive the last line from the second, we make the change of variable $x=2\alpha r$. For the kinetic energy

$$\begin{aligned}&-\frac{1}{2\mu}\int_0^\infty \chi_n(r)\frac{d^2}{dr^2}\chi_m(r)dr\\ &\quad=-\frac{1}{2\mu}\left(\chi_n(r)\frac{d}{dr}\chi_m(r)|_0^\infty-\int_0^\infty\frac{d}{dr}\chi_n(r)\frac{d}{dr}\chi_m(r)dr\right)\\ &\quad=\frac{1}{2\mu}\int_0^\infty\frac{d}{dr}\chi_n(r)\frac{d}{dr}\chi_m(r)dr\\ &\quad=\frac{1}{2\mu}\int_0^\infty\frac{d}{dr}e^{-\alpha r}\tilde{\chi}_n(r)\frac{d}{dr}e^{-\alpha r}\tilde{\chi}_m(r)dr\\ &\quad\approx\frac{1}{2\mu}\sum_i^N\left(\frac{d}{dr}\tilde{\chi}_n(r_i)-\alpha\tilde{\chi}_n(r_i)\right)\\ &\qquad\times\left(\frac{d}{dr}\tilde{\chi}_m(r_i)-\alpha\tilde{\chi}_m(r_i)\right)w_i\end{aligned} \tag{9}$$

where we dropped the surface term at $r=0$ because we will drop that DVR point if we are using one element on $[0,\infty)$ or because it will cancel when we append a Laguerre finite element on $[R_0,\infty)$ to Lobatto DVR

in a finite element ending at R_0, and we drop the surface term at ∞ because the DVR functions $\chi_n(r)$ go to zero at that limit. To get the last line we again make the change of variable $x = 2\alpha r$, to get the weight function to be e^{-x} and then apply ordinary Laguerre quadrature. Note that the derivative terms of the kinetic energy aren't being quadratured exactly for this DVR, as it is for the Lobatto-type DVR based on Gauss-Legendre quadrature. The reason is that three the terms in the product $\left(\frac{d}{dr}\tilde{\chi}_n(r_i) - \alpha\tilde{\chi}_n(r_i)\right)\left(\frac{d}{dr}\tilde{\chi}_m(r_i) - \alpha\tilde{\chi}_m(r_i)\right)$ are of maximum order $2N-1$ or $2N$. The Gauss-Radau quadrature does $2N-2$ exactly. The centrifugal potential is always quadratured approximately in any ordinary DVR because it's not a polynomial.

We can simplify the final working expression for the kinetic energy matrix elements using the properties of the so-called "cardinal functions" $\tilde{\chi}_n$,

$$\begin{aligned}
&\text{Real coordinates}\\
T_{nm} &= -\frac{1}{2\mu}\int_0^\infty \chi_n(r)\left(\frac{d^2}{dr^2} + \frac{l(l+1)}{2\mu r^2}\right)\chi_m(r)dr\\
&\approx \frac{1}{2\mu}\sum_i^N w_i\tilde{\chi}_n'(r_i)\tilde{\chi}_m'(r_i) + \delta_{n,m}\frac{\alpha^2}{2\mu}\\
&- \frac{\alpha}{2\mu}\sqrt{w_n}\tilde{\chi}_m'(r_n) - \frac{\alpha}{2\mu}\sqrt{w_m}\tilde{\chi}_n'(r_m)\\
&+ \frac{l(l+1)}{2\mu r_n^2}\delta_{n,m}\\
V_{n,m} &= \int_0^\infty \chi_n(r)V(r)\chi_m(r)dr = \delta_{n,m}V(r_n)
\end{aligned} \tag{10}$$

where the derivatives $\tilde{\chi}_n'$ are those of the functions $\tilde{\chi}_n$ defined in Eq.(3).

II. POINTS, WEIGHTS AND MATRIX ELEMENTS FOR A DVR FINITE ELEMENT ON THE *REAL* INTERVAL $[R_0, \infty)$

Now we shift the functions, which redefines the DVR quadrature points in terms of the unscaled Laguerre-Radau points and weights,

$$\begin{aligned}
\chi_n(r) &= e^{-\alpha(r-R_0)}\tilde{\chi}_n(r)\\
\tilde{\chi}_n(r) &= \frac{1}{\sqrt{w_n}}\prod_{i\neq n}^N \frac{r-r_i}{r_n-r_i}\\
r_i &= \frac{x_i}{2\alpha} + R_0\\
w_i &= \frac{W_i}{2\alpha}
\end{aligned} \tag{11}$$

These functions are to be appended to the ordinary FEM-DVR grid with the point $r_1 = R_0$ at the end of the other elements. That means that only the first Laguerre DVR function is nonzero at $r = R_0$,

$$\begin{aligned}
\chi_n(R_0) = \chi_n(r_1) &= 0 \text{ for } n \neq 1\\
\chi_1(R_0) = \chi_1(r_1) &= 1/\sqrt{w_1}
\end{aligned} \tag{12}$$

so the last "bridging function" is built as the others are by adding the weights from the right and left elements at the boundary.

The integrals we have to do now to build the parts of the Hamiltonian matrix that we append to the ordinary Gauss-Lobatto FEM-DVR Hamiltonian in the usual way, with the bridging function defined to be a Gauss-Lobatto function on the left of R_0 and a Gauss-Radau Laguerre function on the right of R_0 are

$$\begin{aligned}
V_{n,m} &= \int_{R_0}^\infty \chi_n(r)V(r)\chi_m(r)dr\\
T_{nm} &= -\frac{1}{2\mu}\int_{R_0}^\infty \chi_n(r)\left(\frac{d^2}{dr^2} + \frac{l(l+1)}{2\mu r^2}\right)\chi_m(r)dr
\end{aligned} \tag{13}$$

Next we make the change of variable $r = x/2\alpha + R_0$ to get the weight function to be e^{-x} and the interval to be $[0,\infty)$ in both of these so we can apply ordinary Laguerre quadrature.

The equations for the matrix elements then come out to be exactly the ones in Eq.(10), but with the points and weights defined as in Eq.(11).

III. POINTS, WEIGHTS AND MATRIX ELEMENTS FOR A DVR FINITE ELEMENT ON THE *ECS* INTERVAL $[R_0, \infty e^{i\theta})$

Choosing the right DVR basis functions for ECS with the Laguerre quadrature is a little more subtle that for our usual Gauss-Lobatto FEM-DVR. In that case we just place the DVR points on the complex ECS portion of the contour by scaling the finite interval $[a,b]$ onto the contour. The weights are then automatically scaled by factor $e^{i\theta}$ and the cardinal functions

$$\prod_{i\neq n}^N \frac{r-r_i}{r_n-r_i} \tag{14}$$

have the property that they are *real-valued* for points r on the contour. The way we define our DVR basis functions with a factor of $1/\sqrt{w_n}$ is the only thing that makes them complex on the ECS contour, and that is a matter of convenient normalization and doesn't change anything.

If we do that in the case of the Laguerre DVR cardinal functions they become intrinsically complex on the ray because of the exponential prefactor. The correct way to

define them is

$$\begin{aligned}\chi_n(r) &= e^{-\alpha e^{-i\theta}(r-R_0)}\tilde{\chi}_n(r)\\ \tilde{\chi}_n(r) &= \frac{1}{\sqrt{w_n}}\prod_{i\neq n}^{N}\frac{r-r_i}{r_n-r_i}\\ r_i &= e^{i\theta}\frac{x_i}{2\alpha}+R_0\\ w_i &= \frac{e^{i\theta}W_i}{2\alpha}\end{aligned} \tag{15}$$

With this definition the DVR basis functions are real on the ECS contour except for the overall $1/\sqrt{w_n}$ normalization factor. They are plotted in Fig. 1 for a low order case.

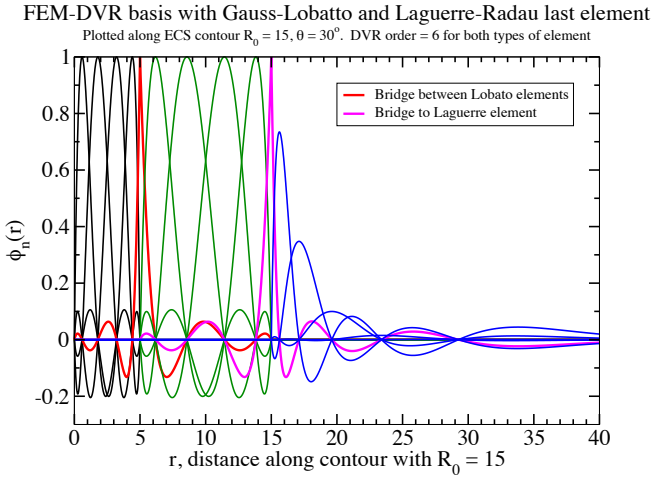

FIG. 1. 6th order DVR with boundaries at $r = 0, 5, 15$, and a 6th order Laguerre element beyond that. Laguerre exponent is $\alpha = 0.5$. On the contour all the functions are real.

To see that this is the correct definition that in fact can be mapped onto ordinary Laguerre quadrature with a weight function of e^{-x} consider the potential matrix elements, which for $V = 1$ give us the overlap matrix elements. Going back to the original FEM-DVR paper [2], we see that the matrix elements are given by the contour integral,

$$\begin{aligned}V_{n,m} &= \int_{R_0}^{\infty e^{i\theta}}\chi_n(z)V(z)\chi_m(z)dz\\ &= \int_{R_0}^{\infty e^{i\theta}}\tilde{\chi}_n(z)V(z)\tilde{\chi}_m(z)e^{-2\alpha e^{-i\theta}(z-R_0)}dz\\ &= \int_0^{\infty}\tilde{\chi}_n\left(\frac{xe^{i\theta}}{2\alpha}+R_0\right)V\left(\frac{xe^{i\theta}}{2\alpha}+R_0\right)\\ &\quad\times\tilde{\chi}_m\left(\frac{xe^{i\theta}}{2\alpha}+R_0\right)\,e^{-x}\,dx\frac{e^{i\theta}}{2\alpha}\\ &\approx \cdot\sum_i w_i\tilde{\chi}_m(r_i)V(r_i)\tilde{\chi}_n(r_i)\\ &= \delta_{n,m}V(r_n)\end{aligned} \tag{16}$$

with w_i ane r_i defined in Eq.(15). The change of variable $r = \frac{xe^{i\theta}}{2\alpha}+R_0$ is the key point because it maps the interval onto $[0,\infty e^{i\theta})$ and the weight function onto the real-valued e^{-x}.

The kinetic energy matrix elements require similar but longer algebra. It is equivalent to what we did for real coordinates but with $\alpha\to\alpha e^{-i\theta}$. So the final working equations for the matrix elements of the Hamiltonian w.r.t. the ECS Laguerre-Radau DVR basis functions are,

On ECS contour

$$\begin{aligned}T_{nm} &= -\frac{1}{2\mu}\int_{R_0}^{\infty e^{i\theta}}\chi_n(z)\left(\frac{d^2}{dz^2}+\frac{l(l+1)}{2\mu z^2}\right)\chi_m(z)dz\\ &\approx \frac{1}{2\mu}\sum_i^N w_i\tilde{\chi}_n'(r_i)\tilde{\chi}_m'(r_i)+\delta_{n,m}\frac{\alpha^2e^{-2i\theta}}{2\mu}\\ &\quad-\frac{\alpha e^{-i\theta}}{2\mu}\sqrt{w_n}\tilde{\chi}_m'(r_n)-\frac{\alpha e^{-i\theta}}{2\mu}\sqrt{w_m}\tilde{\chi}_n'(r_m)\\ &\quad+\frac{l(l+1)}{2\mu r_n^2}\delta_{n,m}\\ V_{n,m} &= \int_{R_0}^{\infty e^{i\theta}}\chi_n(z)V(z)\chi_m(z)dz = \delta_{n,m}V(r_n)\end{aligned}$$

$$\begin{aligned}\chi_n(r) &= e^{-\alpha e^{-i\theta}(r-R_0)}\tilde{\chi}_n(r)\\ \tilde{\chi}_n(r) &= \frac{1}{\sqrt{w_n}}\prod_{i\neq n}^{N}\frac{r-r_i}{r_n-r_i}\\ r_i &= e^{i\theta}\frac{x_i}{2\alpha}+R_0\\ w_i &= \frac{e^{i\theta}W_i}{2\alpha}\end{aligned} \tag{17}$$

The primes denote derivatives as above, and x_i and W_i are the Laguerre-Radau points and weights for the real interval $[0,\infty)$. These formulas are evidently also correct when R_0 is complex-valued, so they can be used to append a Laguerre element to Gauss-Lobatto elements appearing earlier on complex portion of the ECS contour, if that turns out to be desireable for some reason.

As an aside: in my code for checking that all this works, I build the kinetic energy without the $1/\sqrt{w_n}$ factor in the shape functions, and then divide the result by the proper product of square roots of the weights. So what is programmed there is:

$$\begin{aligned}\sqrt{w_n}\sqrt{w_m}T^{(l=0)}{}_{nm} &\approx \frac{1}{2\mu}\sum_i^N w_i\tilde{\chi}_n'(r_i)\tilde{\chi}_m'(r_i)+\delta_{n,m}w_n\frac{\alpha^2e^{-2i\theta}}{2\mu}\\ &\quad-\frac{\alpha e^{-i\theta}}{2\mu}w_n\tilde{\chi}_m'(r_n)-\frac{\alpha e^{-i\theta}}{2\mu}w_m\tilde{\chi}_n'(r_m)\end{aligned} \tag{18}$$

IV. NUMERICAL TESTS

Just because it's a case with a low energy resonance, and one expects that this idea would have advantages primarily at low energies, these checks were done with the Yukawa potential

$$V(r) = -4.25\frac{e^{-r/2.5}}{r} \tag{19}$$

where the odd-looking parameters were tuned to put a low energy resonance in $l = 2$. The potential is shown Fig. 2.

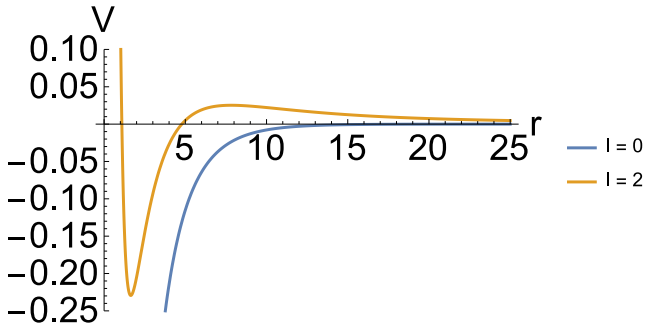

FIG. 2. Test Yukawa potential, $V = -4.25e^{-r/2.5}/r$ that has an $l = 2$ resonance at low energy.

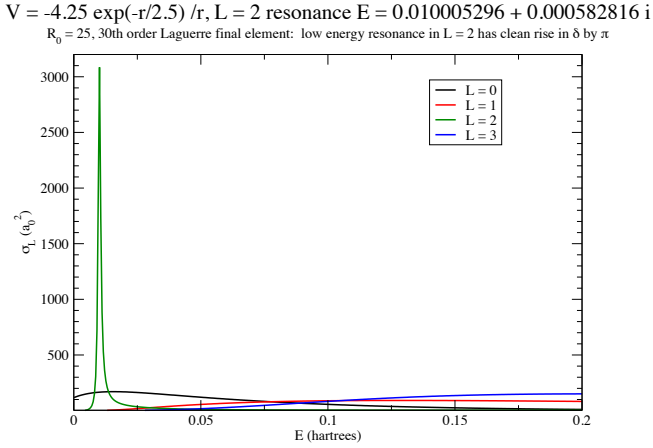

FIG. 3. Partial cross sections for test potential computed with Laguerre element, and converged to far better than graphical accuracy with 15th order DVR with boundaries at $r = 0, 5, 10, 15, 25$, and a 30th order Laguerre element beyond that. The resonance is at 0.100052966E-01 -0.5828158E-03 i (with uncertainty in the last figure from unsystematic convergence study). Laguerre exponent is $\alpha = 0.5$.

The first thing we notice is that adding a Laguerre element puts more complex continuum eigenvalues near $E = 0$ than the pure Gauss-Lobatto grids seem to produce. The bottom line seems to be that adding the Laguerre element requires substantially fewer points to converge the cross section at low energies than does the addition of Gauss-Lobatto elements, as can be seen in Fig. 4.

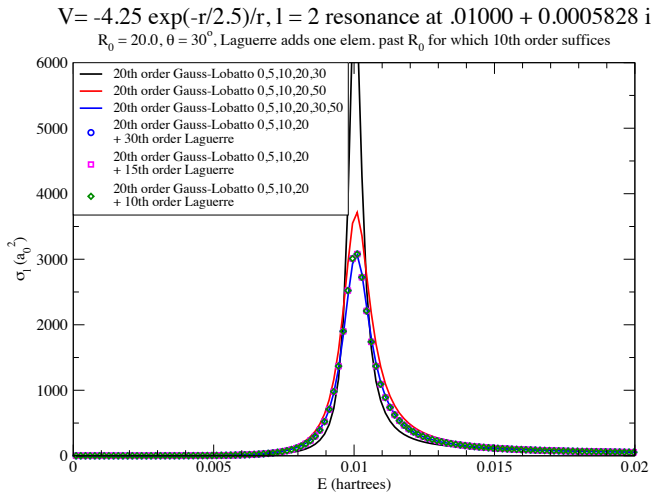

FIG. 4. Comparison of convergence near low energies for $l = 2$ with Gauss-Lobatto DVRs, and with three grids built by adding Laguerre elements of different orders to the first three elements of the Gauss-Lobatto grids only. The Laguerre exponent is $\alpha = 0.5$. The bottom line is that a 10th or 15th order Gauss-Laguerre element is basically always sufficient to converge the cross section if the Laguerre exponent is chosen between about 0.1 and 0.5.

I haven't done an exhaustive exploration of the convergence behavior, but the Gauss-Radau Laguerre DVR seems to be some advantages over our standard Gauss-Lobatto approach, and no disadvantages that I've found so far. There is clearly a trade off between Laguerre DVR order and Laguerre exponent, as seen in Fig. 6 that could be used to optimize the ECS complex final element.

The Laguerre grid also works well for the Coulomb + short range case, and possibly with much smaller grids to reproduce earlier calculations at low energies as shown in Fig. 7.

V. SOLVING POISSON'S EQUATION WITH A RADAU TAIL (ADDED BY FY, JUNE 2018, MODIFIED BY CWM, JULY, 2018)

The preceding tests for appending the Radau tail were on one-electron problems. However, in order to calculate two-electron matrix elements (and single-center expansion integrals such as the nuclear potential of a molecule like H_2) as we do with the FEM-DVR pure Lobatto quadrature, we need to modify the formulation for two-electron radial matrix elements with the Radau tail.

The current evaluation of two-electron radial integrals using the Gauss-Lobatto FEM DVR basis (the angular integrals involving Gaunt coefficients proceeds as before) is based on solving Poisson's equation. The derivation is explained in the ECS topical review, [3]. To calculate

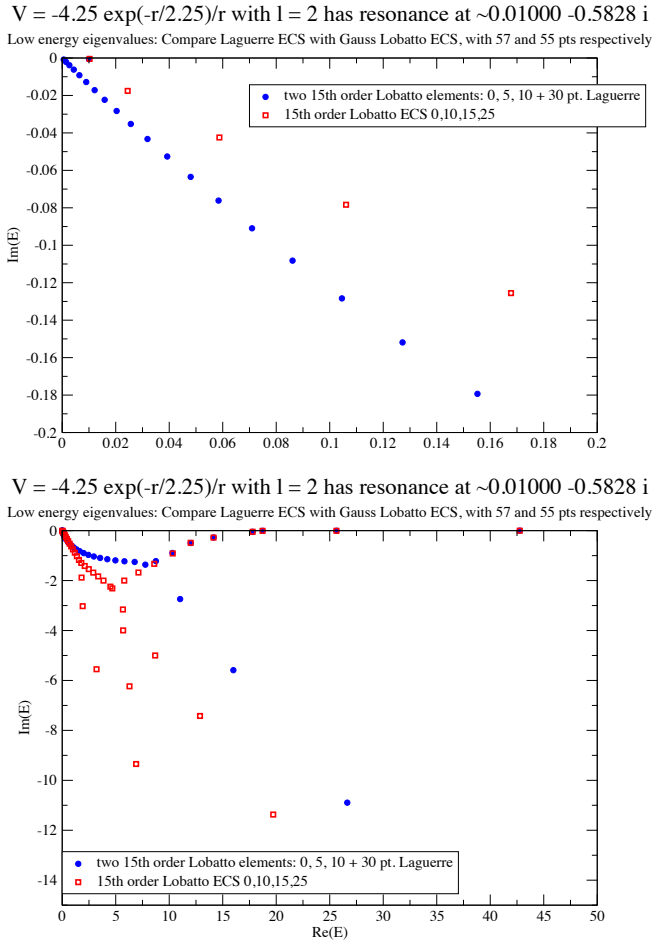

FIG. 5. Comparison of Hamiltonian eigenvalues for grids with and without the Laguerre final element. Grids have the same real-valued elements and the Gauss-Lobatto grid has two additional complex elements with the same number of points as on the Laguerre final element in the other grid. Laguerre exponent is $\alpha = 0.5$.

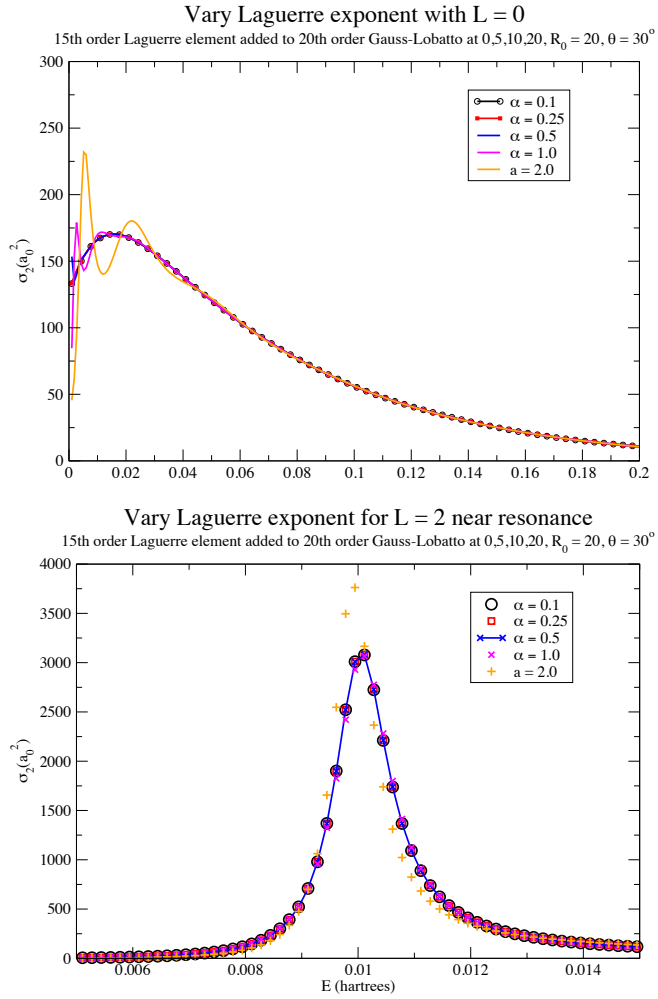

FIG. 6. Varying the Laguerre exponent α with a fixed small number of DVR grid points (here 15) does make a difference at low energies, but values between $\alpha = 0.1$ and $\alpha = 0.5$ work down to less than 0.01 hartree.

the radial part of the two-electron matrix element,

$$\left\langle \rho_B \left| \frac{r_<^\ell}{r_>^{\ell+1}} \right| \rho_A \right\rangle = \int_0^{\infty e^{i\theta}} dr \int_0^{\infty e^{i\theta}} dr' \rho_B(r) \frac{r_<^\ell}{r_>^{\ell+1}} \rho_A(r') \tag{20}$$

where the densities $\rho_A(r)$ and $\rho_B(r)$ are products of radial FEM-DVR Gauss - Lobatto basis functions

$$\rho_A(r) = \phi_i(r)\phi_k(r) \tag{21}$$
$$\rho_B(r) = \phi_j(r)\phi_l(r). \tag{22}$$

In the case of the current *Gauss-Lobatto FEM-DVR*, the final FEM right endpoint provides the upper boundary for the radial integration, with the boundary conditions enforced by discarding the first and last basis functions corresponding to the endpoints, $[0, b]$. Defining the function $y(r)$

$$y(r) = r \int_0^b \rho_A(r') \frac{r_<^\ell}{r_>^{\ell+1}} dr' \tag{23}$$

so that the finite-range integral can be written as a (Lobatto) quadrature

$$\left\langle \rho_B \left| \frac{r_<^\ell}{r_>^{\ell+1}} \right| \rho_A \right\rangle = \int_0^b \rho_B(r) \frac{1}{r} y(r) dr. \tag{24}$$

Differenting $y(r)$ with respect to r shows that it satisfies the radial form of Poisson's equation

$$\left(\frac{d^2}{dr^2} - \frac{\ell(\ell+1)}{r^2} \right) y(r) = -\frac{2\ell+1}{r} \rho_A(r) \tag{25}$$

with, the boundary condition at finite b endpoint

$$y(b) = \frac{1}{b^\ell} \int_0^b \rho_A(t) t^\ell dt = \frac{1}{b^\ell} \delta_{i,k} r_i^\ell \tag{26}$$

where the integral is evaluated with Lobatto quadrature using the properties of the DVR basis functions.

To derive the formula for the two electron matrix elements we first expand the solution of Poisson's equation

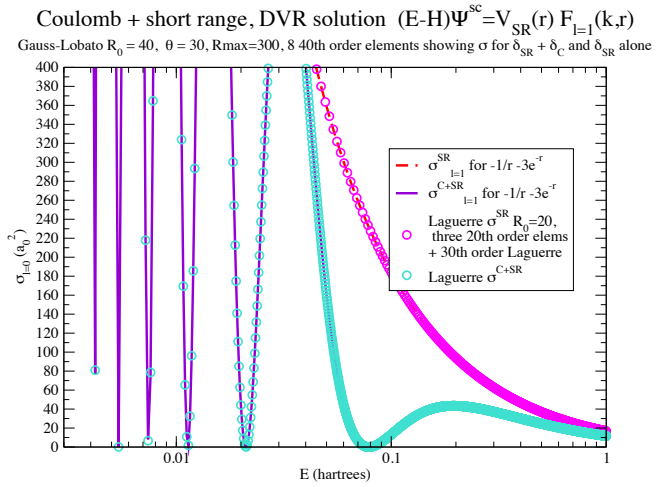

FIG. 7. Reproduced earlier very low energy Coulomb + Short Range potential results using only 3 Gauss-Lobatto elements + 30th order Laguerre element with $\alpha = 0.3$. This was a much smaller grid with the last Laguerre DVR point at ≈ 340, but I don't know if the earlier Gauss-Lobatto grid was an overkill.

in the DVR basis functions

$$y(r) = \sum_m C_m \phi_m(r) \tag{27}$$

and solve for the C_m coefficients, which become

$$C_m = (2\ell+1)\left[T^{(\ell)}_{m,i}\right]^{-1} \frac{1}{r_i w_i^{1/2}} \delta_{ik} \tag{28}$$

where $\left[T^{(\ell)}_{m,i}\right]^{-1}$ is the m,i element of the matrix inverse of twice the kinetic energy. Then we add a solution to the homogeneous equation that enforces the correct boundary conditions at the last DVR point, whose Lobatto shape function we have left out. The solution in Eq.(27) is thus zero at that point, and so if we add a constant times the solution of the homogeneous equation that is regular at the origin ($r^{\ell+1}$), we can enforce the correct boundary condition at $r = r_{max}$, which is the complex value of r at the end of the ECS grid,

$$y(r) = \sum_m C_m \phi_m(r) + r^{\ell+1} r_i^\ell / r_{max}^{2\ell+1} \tag{29}$$

Then, following the derivation in [3], the final result for Lobatto FEM-DVR is

$$\left\langle \chi_j \chi_l \left| \frac{r_<^\ell}{r_>^{\ell+1}} \right| \chi_i \chi_k \right\rangle = \delta_{j,l}\delta_{i,k} \left(\frac{(2\ell+1)}{r_j\sqrt{w_j} r_i \sqrt{w_i}} \left[T^{(\ell)}_{j,i}\right]^{-1} + \frac{r_i^\ell r_j^\ell}{r_{max}^{2\ell+1}} \right), \tag{30}$$

Appending the Laguerre-Radau DVR finite element on $[R_0, \infty e^{i\theta}]$ changes the nature of the basis, so that all the functions satisfy the boundary condition $\phi_m(r) \underset{r\to\infty}{\longrightarrow} 0$, rather than vanishing at a finite value of $r = b$.

The boundary conditions on $y(r)$ in Eq.(25) can be deduced from equations 55a and 55b or equation 59 in the topical review [3]. They are

$$\begin{aligned} y(0) &= 0 \\ y(r) &\underset{r\to\infty}{\longrightarrow} \frac{1}{r^\ell} \int_0^\infty \rho_A(t) t^\ell dt \end{aligned} \tag{31}$$

Our basis of functions $\{\phi_n(r)\}$ satisfies the first of these conditions and goes to zero exponentially on the infinite Laguerre portion of the contour, as can be seen explicitly in Eq.(32). We have no immediately obvious way to correct the boundary conditions they impose, which is simply wrong for $\ell = 0$ and goes to zero with the wrong functional form for $\ell \neq 0$.

So here we will try two approaches. The first following, in Section V A, is exactly the original Poisson equation approach in the Topical Review without applying a boundary condition correction. That's a numerical experiment that Frank Yip did, as explained below. The second approach, described below in Section V B, starts with a different version of the Poisson equation and a redefinition of $y(r)$ that goes to zero at large r for *all* ℓ.

A. Gauss-Lobatto FEM DVR grid with added Laguerre-Radau element and no boundary condition correction

To use the FEM-DVR with a Radau tail, we need to modify the kinetic energy inverse to incorporate the weight function for the integral over the interval $[0, \infty e^{i\theta})$, and it will appear in the solution of Poisson's equation. However we have to rederive the solution of Eq.(25), because the integrals with three DVR basis functions, have either three functions without the exponential Laguerre weight, or three functions with those exponential weighting functions.

First we define the global DVR basis with bridging functions and the appropriate weights for the functions on the Laguerre-Radau ECS tail, using the notation of the topical review [3]. For Mth order Laguerre-Radau quadrature there will be M basis functions of the form given in Eq.(15)

$$\begin{aligned} \chi_n(r) &= e^{-\alpha e^{-i\theta}(r-R_0)} \tilde{\chi}_n(r) \\ \tilde{\chi}_n(r) &= \frac{1}{\sqrt{w_n}} \prod_{i\neq n}^{N} \frac{r - r_i}{r_n - r_i} \\ r_i &= e^{i\theta} \frac{x_i}{2\alpha} + R_0 \\ w_i &= \frac{e^{i\theta} W_i}{2\alpha} \end{aligned} \tag{32}$$

If there is a total of N Gauss-Lobatto *excluding* the one forming half the bridging function that is nonzero at $r =$

r_0, then the single DVR basis defined after Eq.(48) in [3] is $\{\phi_1, \phi_2, \cdots, \phi_{N+M}\}$, with functions $\phi_{N+1}, \cdots, \phi_{N+M}$ having the weight function $^{-\alpha e^{-i\theta}(r-R_0)}$. With this numbering the point $r_{N+1} = R_0$. The only point of numbering them this way is to emphasize the fact that the $N+1$st point, namely the quadrature point that samples the function that br idges between the ECS Radau tail and the last Gauss-Lobatto function doesn't have an exponential weight, because the exponential is equals 1 at that point.

We can solve Eq.(25) for $\ell \neq 0$ with the boundary condition that $Y_\ell(r) \to 0$, although not as a reciprocal power of r that by expanding $y(r)$ in our DVR basis. At least for $\ell \neq 0$ that should work in principal although it might require a large number of Laguerre points on the Laguerre-Radau tail of the grid. To work out the algebra for that solution we expand $y(r)$ in the basis as

$$y(r) = \sum_{m=1}^{N+M} C_m \phi_m(r) \tag{33}$$

and it automatically satisfies the right boundary conditions.

Multiplying Eq.(25) by ϕ_n and integrating over r along the contour we have

$$\begin{aligned}\sum_{m=1}^{N+M} T^{(\ell)}_{n,m} C_m \\ = (2\ell+1)\left(\int_0^{R_0} + \int_{R_0}^{+\infty e^{i\theta}}\right)\frac{\phi_n(r)\phi_i(r)\phi_k(r)}{r}dr\end{aligned} \tag{34}$$

where we used the definition $\rho_A(r) = \phi_i(r)\phi_k(r)$. The matrix $T^{(\ell)}_{n,m}$ is 2μ times the kinetic energy. On the Radau tail (the complex part of ECS contour) it is

$$\begin{aligned}T^{(\ell)}_{n,m} &= -\int_{R_0}^{\infty e^{i\theta}} \chi_n(z)\left(\frac{d^2}{dz^2} + \frac{\ell(\ell+1)}{z^2}\right)\chi_m(z)dz \\ &\approx \sum_{i=1}^{M} w_i \tilde{\chi}'_n(r_i)\tilde{\chi}'_m(r_i) + \delta_{n,m}\alpha^2 e^{-2i\theta} \\ &- \alpha e^{-i\theta}\sqrt{w_n}\tilde{\chi}'_m(r_n) - \alpha e^{-i\theta}\sqrt{w_m}\tilde{\chi}'_n(r_m) \\ &+ \frac{\ell(\ell+1)}{r_n^2}\delta_{n,m},\end{aligned} \tag{35}$$

and is combined with the definition for the Gauss-Lobatto blocks for $r \leq R_0$ in the usual way so that the weight for the bridging function is $\sqrt{w_N + w_1^{\text{Lag-Rad}}}$ where $w_1^{\text{Lag-Rad}} = \frac{e^{i\theta}W_1}{2\alpha}$ to form the complete matrix $T^{(\ell)}_{n,m}$. This is what was done in the one-electron formulation and tests above.

Now we have to evaluate the right hand side of Eq.(34). For basis functions ϕ_n up to and *including* the bridging function the factor $e^{-\alpha e^{-i\theta}(r-R_0)}$ does not appear or is unity, so performing the integral with the DVR quadrature gives

$$\begin{aligned}(2\ell+1)\int_0^{\infty e^{i\theta}} \frac{\phi_n(r)\phi_i(r)\phi_k(r)}{r}dr \\ = (2\ell+1)\frac{\delta_{ni}\delta_{ik}}{r_n w_n^{3/2}}w_n = (2\ell+1)\frac{\delta_{ni}\delta_{ik}}{r_n w_n^{1/2}}\end{aligned} \tag{36}$$

but for ϕ_n on the complex part of the contour, $n = N+1, \cdots, M$ we have

$$\begin{aligned}(2\ell+1)\int_0^{\infty e^{i\theta}} \frac{\tilde{\chi}_n(r)\tilde{\chi}_i(r)\tilde{\chi}_k(r)}{r}\left(e^{-\alpha e^{-i\theta}(r-R_0)}\right)^3 dr \\ = (2\ell+1)\frac{\delta_{ni}\delta_{ik}}{r_n w_n^{3/2}}w_n\left(e^{-\alpha e^{-i\theta}(r_n-R_0)}\right)^1 \\ = (2\ell+1)\frac{\delta_{ni}\delta_{ik}e^{-\alpha e^{-i\theta}(r_n-R_0)}}{r_n w_n^{1/2}}\end{aligned} \tag{37}$$

because the Radau-Laguerre quadrature has the weight $e^{-2\alpha e^{-i\theta}(r-R_0)}$ (note the factor of 2α in the exponent).

The equation for $y(r)$ now reads

$$\begin{aligned}&\sum_{m=1}^{N+M} T^{(\ell)}_{n,m} C_m = d_n\delta_{ik} \\ &d_n = \\ &\begin{cases}(2\ell+1)\frac{\delta_{ni}}{r_i w_i^{1/2}} & n = 1, \cdots, N \\ (2\ell+1)\frac{\delta_{ni}}{r_i w_i^{1/2}}e^{-\alpha e^{-i\theta}(r_i-R_0)} & n = N+1, \cdots, M\end{cases}\end{aligned} \tag{38}$$

So the solution for $y(r)$ is

$$\begin{aligned}&y(r) = \sum_{m=1}^{N+M} C_m\phi_m(r) \\ &C_m = (2\ell+1)\left[T^{(\ell)}_{m,i}\right]^{-1} d_i\delta_{ik} \\ &d_i = \begin{cases}\frac{1}{r_i w_i^{1/2}} & i = 1, \cdots, N \\ \frac{1}{r_i w_i^{1/2}}e^{-\alpha e^{-i\theta}(r_i-R_0)} & i = N+1, \cdots, M\end{cases}\end{aligned} \tag{39}$$

We now return to Eq.(24) for the radial two-electron integral, and perform the integral using the DVR quadrature

$$\left\langle \rho_B \left| \frac{r_<^\ell}{r_>^{\ell+1}} \right| \rho_A \right\rangle = \left(\int_0^{R_0} + \int_{R_0}^{+\infty e^{i\theta}}\right)\rho_B(r)\frac{1}{r}y(r)dr. \tag{40}$$

and use the definition

$$\rho_B(r) = \phi_j(r)\phi_l(r) \tag{41}$$

That gives us the integral

$$\left\langle \rho_B \left| \frac{r_<^\ell}{r_>^{\ell+1}} \right| \rho_A \right\rangle = \int_0^{R_0} \chi_j(r)\chi_l(r)\frac{1}{r}y(r)dr + \int_{R_0}^{+\infty e^{i\theta}} \tilde{\chi}_j(r)\tilde{\chi}_l(r)\frac{1}{r}y(r)e^{-2\alpha e^{-i\theta}(r-R_0)}dr \tag{42}$$

where writing the contour integral in two parts explicitly allows us to see that one factor of $e^{-\alpha e^{-i\theta}(r-R_0)}$ comes from each DVR function in ρ_B, but another factor of that weight comes with the basis expansion of $y(r)$.

Now we insert the representation for $y(r)$ on the contour, and return to the more compact notation $\int_0^{+\infty e^{i\theta}}$

$$\begin{aligned}\left\langle \rho_B \left| \frac{r_<^\ell}{r_>^{\ell+1}} \right| \rho_A \right\rangle &= \sum_{m=1}^{N+M} C_m \int_0^{+\infty e^{i\theta}} \phi_j(r)\phi_l(r)\frac{1}{r}\phi_m(r)dr \\ &= \sum_{m=1}^{N+M} C_m d_j \delta_{jl},\delta_{mj} \\ &= (2\ell+1)\sum_{m=1}^{N+M}\left[T^{(\ell)}_{m,i}\right]^{-1} d_i\delta_{ik}\ d_j\delta_{jl}\ \delta_{mj}\end{aligned} \tag{43}$$

We performed this integral with the DVR quadrature, and the exponential Laguerre weights $e^{-2\alpha e^{-i\theta}(r_i-R_0)}$ are included in the quadrature, so again an extra factor of $e^{-\alpha e^{-i\theta}(r_i-R_0)}$ is introduced by this integration for the points where r_i is complex. The integral is exactly the same as the one in Eqs.(36-37). The sum over m is done with the Kronecker δ_{jm}.

The final result has the symmetric form we expect

$$\boxed{\begin{aligned}&\left\langle \rho_B \left| \frac{r_<^\ell}{r_>^{\ell+1}} \right| \rho_A \right\rangle = (2\ell+1)\ d_j\left[T^{(\ell)}_{j,i}\right]^{-1} d_i\ \delta_{ik}\delta_{jl} \\ &d_i = \begin{cases} \frac{1}{r_i w_i^{1/2}} & i=1,\cdots,N \\ \frac{1}{r_i w_i^{1/2}} e^{-\alpha e^{-i\theta}(r_i-R_0)} & i=N+1,\cdots,M \end{cases}\end{aligned}} \tag{44}$$

but no boundary terms so far to enforce the correct boudary conditions on $y(r)$.

Frank Yip found that adding the term

$$\frac{r_j^\ell r_i^\ell}{b^{2\ell+1}} \qquad with \qquad b = \frac{2M}{\alpha e^{-i\theta}} + R_0 \tag{45}$$

produces the correct result to 14 significant figures when $\ell = 0$ for the integrals when ρ_A and ρ_B are on the real part of the ECS contour. For other values of ℓ it produces a minimum of 5 figures ($\ell = 1$) and does successively better for higher ℓ values until at $\ell = 3$ it's accurate to 14 figures again. The question is: why?

To see what this correction is doing we can go back to Poisson's equation and see how adding the homogeneous solution that corresponds to this correction to the two electron integrals affects the solution. So we now write our solution as

$$\begin{aligned} y(r) &= \sum_{m=1}^{N+M} C_m\phi_m(r) + \frac{r_i^\ell r^{\ell+1}}{b^{2\ell+1}} \\ C_m &= (2\ell+1)\left[T^{(\ell)}_{m,i}\right]^{-1} d_i\delta_{ik} + r_i^\ell \\ b &= \frac{2M}{\alpha e^{-i\theta}} + R_0 \end{aligned} \tag{46}$$

Note the the first sum in this equation for $y(r)$ is complex everywhere, but y(r) has to be real, at least on the real part of the ECS contour.

Before plotting $y(r)$ from various solutions of Poisson's equation, it's useful to look at how the Laguerre-Radau FEM DVR grid approximates functions when we interpolate them with this basis. To do so we expand them according to

$$\begin{aligned} y(r) &= \sum_m C_m\phi_m(r) \\ C_m &= y(r_m)w_m \ \text{ or } \ \ y(r_m)w_m e^{+\alpha e^{-i\theta} r_m} \end{aligned} \tag{47}$$

Fig. 8 shows how well that works for the functions

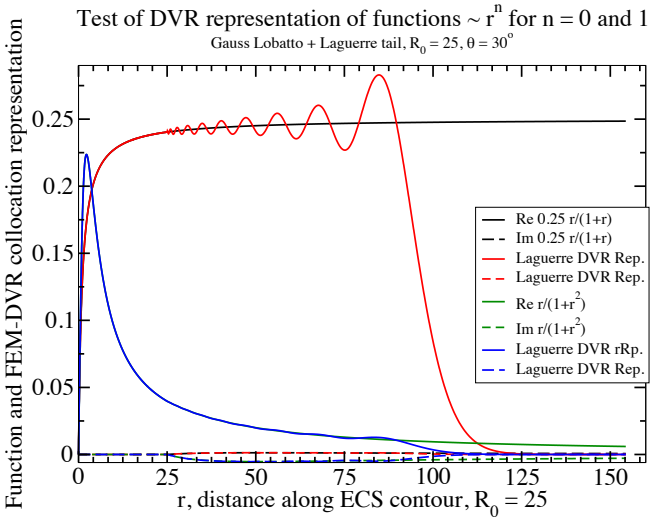

FIG. 8. Approximating functions that limit to constants or fall off like $1/r$ with the Laguerre FEM DVR grid using collocation.

To see how adding the homogeneous solution to $y(r)$ works in both the Gauss-Lobatto ECS approach that we have used before and Laguerre-Radau grid we are using here, we need to plot the contributions to$y(r)$ in both cases and compare them. That's done in Fig. 9 for the functions $r/(1+r)$ and $r/(1+r^2)$, which go to a constant or fall off like $1/r$. The difficulties with this representation, which is pretty good except for when we try to represent a constant in terms of exponentially decaying functions, are apparent. It's worth noting that this test works essentially to machine accuracy for functions that go asymptotically like e^{ikr} which decay exponentially on the ECS grid.

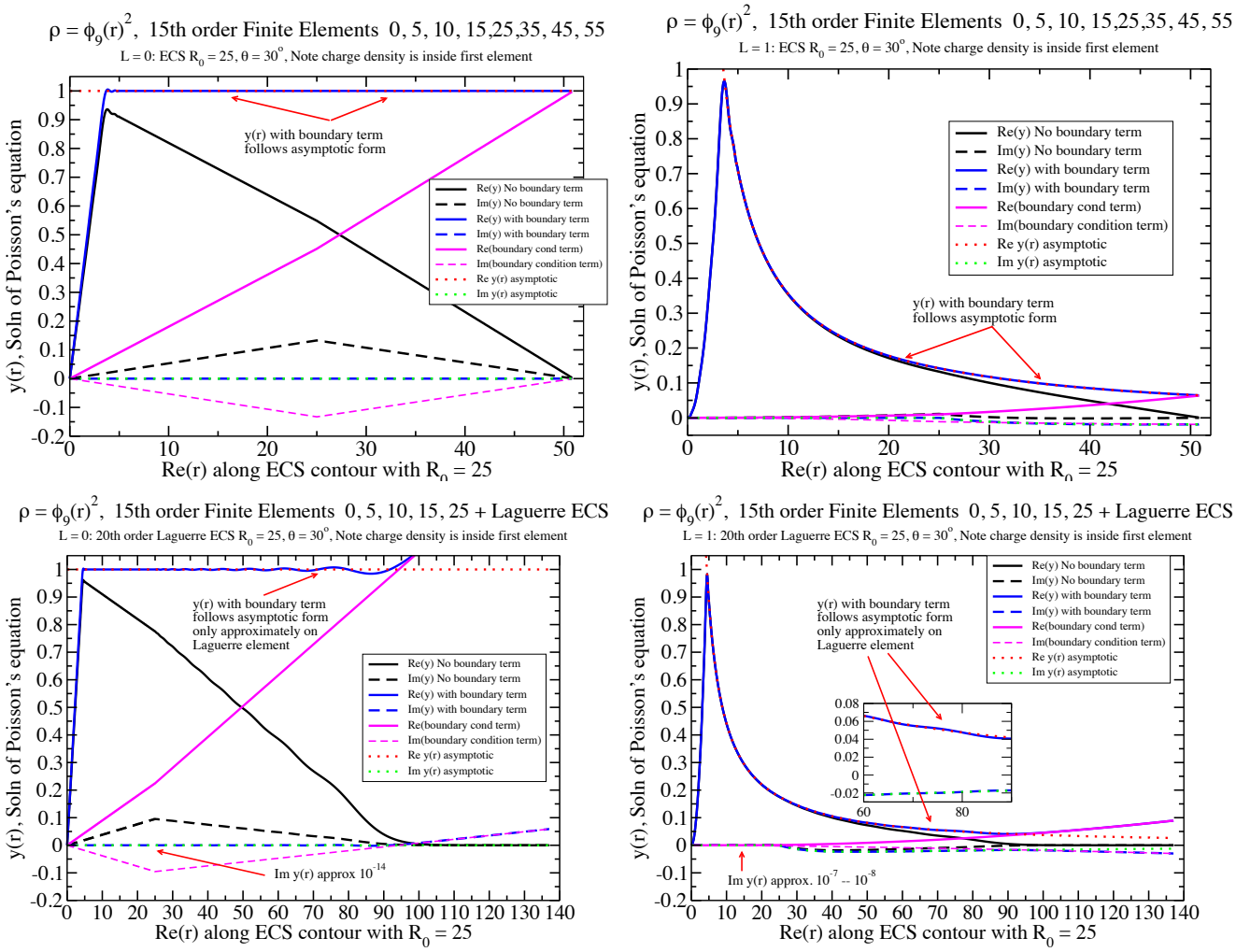

FIG. 9. Solutions of Poisson's equation for $\ell = 0$ and $\ell = 1$ using both the Gauss-Lobatto FEM DVR (top row) and the Laguerre-Radau FEM DVR (bottom row). The driving term $(2\ell + 1)\rho_A(r)/r$ is the same in all cases, and is a density in the first real element of the ECS contour. The real parts of the grids are the same, and Laguerre exponent is $\alpha = 0.5$. Other parameters are in the figures themselves. The $y(r)$ solutions with the boundary condition term added are in blue. Note the red and green dotted lines are the real and imaginary parts of the asymptotic form of $y(r)$, and that the Radau-Laguerre grid approach only approximately (although to a very good approximation in most cases) follows that asymptotic form.

We can observe in Fig. 9 that the homogeneous solution enforces the boundary condition on $y(r)$, namely $y(r) \sim r_i^\ell / r^\ell$, essentially exactly in the case of the Gauss-Lobatto FEM DVR. That's true on the complex part of the contour as well where $y(r)$ is complex for nonzero ℓ. The Laguerre-Radau FEM DVR does this only approximately in all cases, particularly on the complex part of the grid. It's best for $\ell = 0$, and worst for $\ell = 1$ but continues to improve for higher ℓ values – just like the values of the two electron integrals on the real part of the contour computed with the Laguerre-Radau approach.

B. Modified Poisson equation approach with solution vanishing at $r \to \infty$ and the $r^2 dr$ volume element

1. Definition of $\tilde{y}(r)$ and the two electron integral in terms of it

We can solve for $\tilde{y}(r)$ defined instead as

$$\tilde{y}(r) = \int_0^\infty \rho_A(r') \frac{r_<^\ell}{r_>^{\ell+1}} r'^2 dr' \tag{48}$$

which modifies the original definition of $y(r)$ in two ways. First an overall factor of r is removed and for reasons that will become clear below, we use the $r^2 dr$ volume element. This function satisfies the boundary conditions,

$$\begin{aligned} \tilde{y}(r) &\underset{r\to 0}{\longrightarrow} r^\ell \int_0^\infty \rho_A(t) t^{(1-\ell)} dt \\ \tilde{y}(r) &\underset{r\to \infty}{\longrightarrow} \frac{1}{r^{\ell+1}} \int_0^\infty \rho_A(t) t^\ell t^2 dt \end{aligned} \tag{49}$$

so in addition to vanishing at large r for all ℓ, which is the behavior we seek, it is also finite ar $r = 0$ for $\ell = 0$, which our basis cannot represent.

Direct differentiation shows $\tilde{y}(r)$ satisfies

$$\left(\frac{1}{r^2} \frac{d}{dr} r^2 \frac{d}{dr} - \frac{\ell(\ell+1)}{r^2} \right) \tilde{y}(r) = -(2\ell+1)\rho_A(r) \tag{50}$$

so that we are solving Poisson's equation for a function that decays faster at large r. Then the two-integral can be evaluated as a DVR quadrature of

$$\left\langle \rho_B \left| \frac{r_<^\ell}{r_>^{\ell+1}} \right| \rho_A \right\rangle = \int_0^\infty \rho_B(r) \tilde{y}(r) r^2 dr. \tag{51}$$

2. Gauss-Radau DVR in the first element and definition of DVR basis

Since $\tilde{y}(0) \neq 0$ for $\ell = 0$ we need to use Bret Esry's Gauss-Radau idea, in which we do not solve for r times the radial wave function, but rather the radial function itself, and so we are solving

$$\left[-\frac{1}{2\mu} \frac{1}{r^2} \frac{d}{dr} r^2 \frac{d}{dr} + \frac{\ell(\ell+1)}{2\mu r^2} + V(r) - E \right] \psi = 0 \tag{52}$$

or its two electron counter part. We redefine the basis functions in everywhere to be

$$\chi_n(r) = \frac{1}{\sqrt{w_n r_n^2}} \prod_{i\neq n}^{N} \frac{r - r_i}{r_n - r_i} = \frac{1}{r_n} \times \text{old fcns} \tag{53}$$

and make the first element a Gauss-Radau element with only the right end fixed. There is then no point at $r = 0$ and the basis functions are all nonzero at the origin. Note that one can do this for all ℓ, and the higher ℓ functions will automatically come to be zero at the origin when we solve for them as scattering or bound states. Note also that the same change apply on the Laguerre-Radau last element. The basis functions there are $1/r_n \times$ old fcns that include the exponential weights.

One then defines the matrix elements of the kinetic energy by

1. integrating by parts in each element

$$\begin{aligned} &\int_0^a \chi_n(r) \frac{1}{r^2} \frac{d}{dr} r^2 \frac{d}{dr} \chi_n(x) r^2 dr \\ &\quad = \int_0^a \chi_n(r) \frac{d}{dr} r^2 \frac{d}{dr} \chi_n(r) dr \\ &\quad = r^2 \chi_m(r) \frac{d\chi_n(r)}{dr}\Big|_0^a - \int_0^a \frac{d\chi_n(r)}{dr} \frac{d\chi_m(r)}{dr} r^2 dr \end{aligned} \tag{54}$$

2. using Gauss-Radau quadrature in the first finite element, with the fixed point at $x = a$ to evaluate the integrals $\int_0^a \frac{d\chi_n(r)}{dr} \frac{d\chi_m(r)}{dr} r^2 dr$. That prescription says all matrix elements of local functions are just $\langle \phi_n | V | \phi_m \rangle = \delta_{nm} V(r_n)$ because the $1/r_n$ factors in the basis functions cancel the volume element. Note Gauss-Radau quadrature won't have a point at $r = 0$.

3. using an ordinary Gauss-Lobatto DVR in all subsequent elements, and using the quadrature to evaluate $\int_a^b \frac{d\chi_n(r)}{dr} \frac{d\chi_m(r)}{dr} r^2 dr$ in each element

4. dropping all the surface terms at the element boundaries, which either vanish (at $r = 0$, because r^2 vanishes there) or cancel between adjacent elements.

3. Final expression for two electron integrals

To solve for $\tilde{y}(r)$ in this basis we expand it as before

$$\begin{aligned} \tilde{y}(r) &= \sum_m C_m \phi_m(r) \\ C_m &= \sum_n T^{-1}_{m,n} \left(\int_0^{\infty e^{i\theta}} \phi_n \rho_A(r) r^2 dr \right) \end{aligned} \tag{55}$$

Now the two electron is given by the quadrature in Eq.(51)

$$\left\langle \rho_B \left| \frac{r_<^\ell}{r_>^{\ell+1}} \right| \rho_A \right\rangle = (2\ell+1) \times \sum_{m,n} \left(\int_0^{\infty e^{i\theta}} \rho_B(r') \phi_m(r') r'^2 dr' \right) [T_{m,n}]^{-1} \left(\int_0^{\infty e^{i\theta}} \phi_n \rho_A(r) r^2 dr \right) \tag{56}$$

which is manifestly symmetric. Evaluating the integrals with the quadrature gives an expression with exactly the same form as at the end of Section V A

$$\boxed{\begin{aligned} &\left\langle \rho_B \left| \frac{r_<^\ell}{r_>^{\ell+1}} \right| \rho_A \right\rangle = (2\ell+1)\ d_j \left[T_{j,i}^{(\ell)} \right]^{-1} d_i\ \delta_{ik}\delta_{jl} \\ &d_i = \begin{cases} \frac{1}{r_i w_i^{1/2}} & i = 1, \cdots, N \\ \frac{1}{r_i w_i^{1/2}} e^{-\alpha e^{-i\theta}(r_i - R_0)} & i = N+1, \cdots, M \end{cases} \end{aligned}} \tag{57}$$

because the redefinition of the basis functions causes a cancelation of the r^2 volume element at the quadrature points, and the same cancelation of weights occurs as before.

We could try to add a homogeneous solution to $y(r)$ to try to correct this to have the analytic $1/r^\ell$ asymptotic form, but the general homogeneous solution to Eq.(50) is $Ar^{-\ell} + Br^{\ell+1}$, and that doesn't give much flexibility. Nonetheless that's what Frank Yip has apparently discovered how to do for $\ell = 0$ in Section V A.

[1] Armin Scrinzi, "Infinite-range exterior complex scaling as a perfect absorber in time-dependent problems," Phys. Rev. A **81**, 053845 (2010).

[2] T. N. Rescigno and C. W. McCurdy, "Numerical grid methods for quantum-mechanical scattering problems," Phys. Rev. A **62**, 032706 (2000).

[3] C W McCurdy, M Baertschy, and T N Rescigno, "Solving the three-body coulomb breakup problem using exterior complex scaling," Journal of Physics B: Atomic, Molecular and Optical Physics **37**, R137 (2004).